Nanotechnology **19** (2008) 115601 (5pp) doi:10.1088/0957-4484/19/11/115601

A photovoltaic device based on a poly(phenyleneethynylene)/SWNT composite active layer

Qian Liu[1,2], Jie Mao[3], Zunfeng Liu[3], Nan Zhang[1,2], Yu Wang[1,2], Liying Yang[1,2], Shougen Yin[1,2] and Yongsheng Chen[3]

[1] Key Laboratory of Display Materials and Photoelectric Devices (Tianjin University of Technology), Ministry of Education, Institute of Material Physics, Tianjin University of Technology, Tianjin 300384, People's Republic of China
[2] Tianjin Key Laboratory for Photoelectric Materials and Devices, Tianjin 300384, People's Republic of China
[3] Key Laboratory for Functional Polymer Materials and Center for Nanoscale Science and Technology, Institute of Polymer Chemistry, College of Chemistry, Nankai University, Tianjin 300071, People's Republic of China

E-mail: sgyin@tjut.edu.cn; and yschen99@nankai.edu.cn

Received 9 September 2007, in final form 20 November 2007
Published 18 February 2008
Online at stacks.iop.org/Nano/19/115601

Abstract
Although research on the use of single walled carbon nanotubes (SWNTs) as the acceptor in polymer photovoltaic cells is currently making great progress, their poor dispersion in a polymer matrix has greatly hindered the overall performance of the devices. Here a novel bulk heterojunction structure based on a poly(phenyleneethynylene)/SWNT composite was designed to improve the dispersion of SWNTs in the composite based on their structural similarity and strong interaction. Better dispersion and higher performance are achieved compared with a common control device based on a poly(3-octylthiophene)/SWNT composite layer.

(Some figures in this article are in colour only in the electronic version)

1. Introduction

Polymer photovoltaic cells are becoming increasingly attractive because they show many potential advantages over the traditional silicon-based ones. Solution processing of polymeric materials leads to the possibility of making large-area thin film solar cells using inexpensive liquid based processing techniques such as spin coating [1], ink jet printing [2], doctor blading [3] and screen printing [4]. In a typical polymer solar cell, the generation of electrical power by the absorption of photons is always a result of the spatial separation of excitons (strongly bound electron–hole pairs) at the donor/acceptor interface. The challenge in these devices is to achieve a large area of interface between donor and acceptor materials in order to dissociate excitons efficiently, whilst simultaneously providing connected pathways by which electrons and holes can be transported to the electrodes within the acceptor and donor materials, respectively. Composite materials comprising a conjugated polymer as the electron donor and inorganic semiconducting nanoparticles as the electron acceptor are attractive for photovoltaic systems since the addition of inorganic semiconducting nanoparticles provides higher carrier mobility than the polymer matrix [5]. Small conjugated molecules such as C_{60} and its derivatives, therefore, have been blended with polymers at a concentration that enables the formation of percolation pathways for electron transport [6]. The performances of photovoltaic devices using poly(3-hexylthiophene-1,3-diyl) (P3HT) and [6, 6]-phenyl-C61-butyric acid methyl ester (PCBM) composite layer have increased dramatically in recent years, reaching a power conversion efficiency (η_p) as high as 6% under AM 1.5 (AM = air mass) simulated solar illumination [7]. Nevertheless, the performance of conjugated polymer/PCBM based solar cells has been limited by some critical internal factors such as low charge carrier mobility, inefficient hoping charge transport, and the presence of structural traps in the form of incomplete pathways in the percolation network for electron transport [8]. Compared with C_{60}, single walled

carbon nanotubes (SWNTs) have many advantages, including high charge mobility, long π–π conjugation and large aspect ratio, and therefore they can be expected to reduce the number of inter-particle hops required for electron extraction and the presence of structural traps, and then can be favorable for charge transfer [9].

However, the advantages of the use of SWNTs in photovoltaic devices are somewhat hindered due to their insolubility and poor dispersion in a polymer matrix. So far, a photovoltaic device using polymer/SWNTs composite film as the active layer does not achieve satisfied power conversion efficiency, one of the important reasons being the poor dispersion of SWNTs in the polymer matrix [10]. This is because the device performance depends not only on the properties of the nano-fillers, but also on their arrangement in the film [11]. Therefore a careful control of the film morphology is highly required. An active layer having well dispersed SWNTs will provide plenty of percolation pathways for electron transfer, and hence improve the device performance. Researchers have tried to use chemical [12] or physical [13] methods to modify carbon nanotubes to improve their solubility in the polymer matrix and have achieved improved efficiencies. Here we report a new physical approach to improve the dispersion of SWNTs in a polymer matrix based on structure design of the polymer molecule.

Poly(phenyleneethynylene) (PPE) is a class of rigid-rod conjugated polymer composed of aromatic rings and alkyne functional groups, which can form a hybrid with SWNTs via π–π stacking interaction [9]. In this study, based on the structural similarity of the large π-system of PPE and the SWNTs wall, we prepared a composite material in which SWNTs are well dispersed in a PPE matrix, and used it as the active layer of a photovoltaic device. Compared with a control device using a poly(3-octylthiophene) (P3OT)/SWNT active layer, a much higher open circuit voltage (V_{oc}) and higher energy conversion efficiency are obtained.

2. Experimental details

2.1. Materials

The SWNTs (having a diameter of 1.2–1.8 nm and length of 1–2 μm [14]) were prepared in our laboratory by a direct current arc-discharge method, and were purified using a previously published method [15]. PPE (poly(2,5-bis(11-(9'-naphthylacetylate)-3,6,9-trioxaundecyl)-1,4-phenylene)), Mw $= 10^4$ g mol^{-1} was synthesized according to our procedures reported earlier [9]. Poly(3-octylthiophene) was purchased from Aldrich. All chemical reagents used in this study were purchased from commercial sources (Alfa, Acros and Aldrich). Indium tin oxide (ITO)-coated glass, $R_s \sim 17\ \Omega\ \square^{-1}$, was purchased from CSG Inc.

2.2. Instruments and measurements

UV–vis–NIR spectra were obtained with a JASCO V-570 spectrometer. Atomic force microscopy (AFM) images were obtained on a Nanoscope IV (Digital Instruments Inc.) using the tapping mode. The current–voltage (I–V) measurements of the photovoltaic devices were carried out on a computer controlled Keithley 2400 Source Measure Unit. A xenon lamp with an AM 1.5 filter was used as the white light source, and the optical power at the sample was 100 mW cm^{-2}. The electrochemical cyclic voltammetry (CV) was carried out on an Ecochemie μAutolab III electrochemical station employing a Pt disk as the working electrode, Ag/Ag$^+$ electrode (0.01 M $AgNO_3$) as the reference electrode, and a Pt wire as the counter electrode. The reference electrode was calibrated with ferrocene ($E_{Fc/Fc^+} = 0.071$ V versus Ag/Ag$^+$). Tetrabutylammonium perchlorate (TBAP) was the supporting electrolyte, and the scan rate was 50 mV s^{-1}. The determination system was bubbled with Ar for 15 min to remove the O_2 before the electrochemical cyclic voltammetry (CV) was carried out.

3. Photovoltaic cell fabrication

Photovoltaic devices were fabricated in the structure of ITO ($\sim$17 $\Omega\ \square^{-1}$)/PEDOT:PSS (30 nm)/PPE:SWNTs (100 nm)/LiF (1 nm)/Al (80 nm) (figure 1). The purified SWNTs were dispersed with the aid of a high-power ultrasonic probe in chloroform (0.2 mg ml^{-1}) and were then blended with the polymer solution in chloroform (20 mg ml$^-$) to make the SWNT/polymer hybrid materials (mass ratio of SWNT/polymer $= 1/100$, $C_{polymer} = 10$ mg ml^{-1}) for device fabrication. The devices were fabricated on 2.5 $\times$ 2.5 cm^2 ITO-coated glass substrates. The ITO was cleaned by ultrasonication and rinsed in deionized water, acetone, and isopropanol. The PEDOT:PSS layer (30 nm) was formed by spin coating (2800 rpm) of a commercial product Baytron P (Bayer AG). The active layer was formed by spin coating (1500 rpm) of a solution of 1 wt% of SWNTs in polymer from a 10 mg ml^{-1} chloroform solution prepared according to the above procedure. LiF (1 nm) and Al (80 nm) was deposited on the active layer by vacuum evaporation under 3 $\times$ 10^{-4} Pa. Eight polymer solar cell devices were fabricated in one piece of ITO glass; the effective area of every cell is 4 mm^2.

4. Results and discussion

The schematic representation of the bulk heterojunction solar cell is shown in figure 1(b), and the logarithmic current density (J) versus the voltage (V) of the PPE/SWNT based photovoltaic cell in dark and under light is plotted in figure 1(c). It can be seen that there is no current response in the dark. Under illumination, we get an open circuit voltage (V_{oc}) of 1.04 V and a current density (J_{sc}) of 0.27 mA cm^{-2}. As a comparison, we prepared a device using pristine PPE as the active layer, the J–V curve of which is also shown in figure 1(c). It can be seen the V_{oc} of the heterojunction device is almost three times that of the pristine polymer diodes (0.38 V), and J_{sc} is two orders of magnitude higher than that of the pristine one (0.002 mA cm^{-2}). The increase both in V_{oc} and J_{sc} can be attributed to the addition of SWNTs. The difference in electron affinity between the donor (PPE) and acceptor (SWNTs) provides a built-in potential that breaks

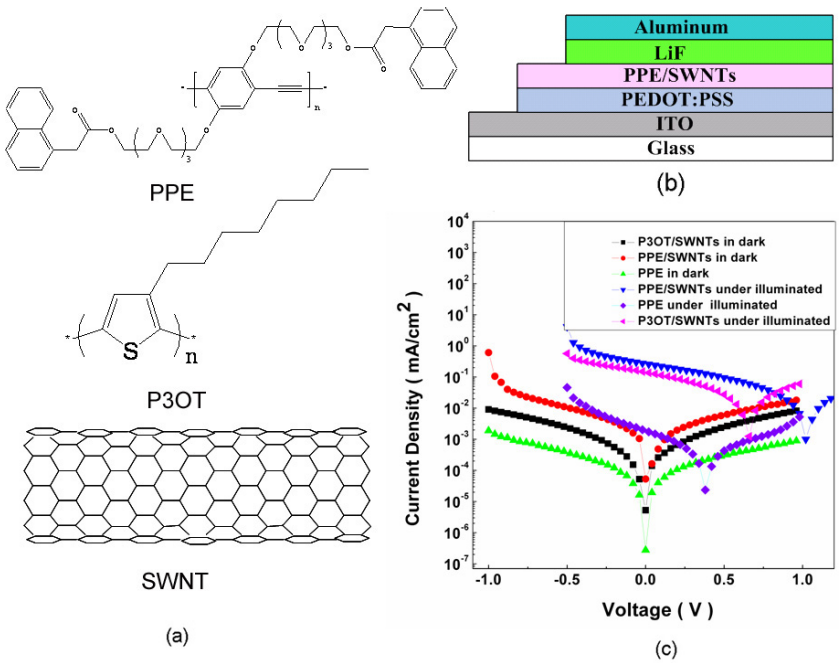

Figure 1. The chemical structure of PPE, P3OT, and an SWNT are shown in the panel (a). A schematic of a device with a PPE/SWNT thin film as the active layer is shown in panel (b): ITO (∼17 Ω $\square^{-1}$)/PEDOT:PSS (30 nm)/PPE:SWNTs (100 nm)/LiF (1 nm)/Al (80 nm). The corresponding logarithmic J–V curves for 100 mW cm^{-2} xenon white light and in the dark of the solar cells on an ITO glass substrate using an active layer of PPE, PPE/SWNTs, and P3OT/SWNTs respectively are shown in panel (c).

the symmetry, and thereby provides a driving force for the dissociation of the photogenerated excitons into electrons and holes [16, 17]. The potential interaction between the highly delocalized π-electrons of carbon nanotubes and the π-electrons correlated with the lattice of the polymer skeleton makes the two species form an interconnecting network and provides a direct pathway for enhanced charge transport and then induces an increased J_{sc}.

In a single-layered organic photovoltaic cell in which the active layer is composed of a pure conjugated polymer, the open circuit voltage V_{oc} is principally determined by the work function difference between the two metal electrodes, i.e. the metal–insulator–metal (MIM) model [18]. The difference between the work function of the ITO electrode (=4.7 eV) and that of the Al cathode (=4.3 eV) is 0.4 eV, which well matches the open circuit voltage (0.4 V) measured on our cell with ITO (∼17 Ω $\square^{-1}$)/PEDOT:PSS (30 nm)/PPE (100 nm)/LiF (1 nm)/Al(80 nm) structure. However, in solar cells having a bulk heterojunction structure, the MIM model is not applicable. For solar cells based on a polymer/SWNT composite, V_{oc} is also influenced by the work function of the SWNTs as well as the highest occupied molecular orbital (HOMO) level of the conjugated polymer [19]. In a controlled device based on a P3OT/SWNT composite layer having a device structure of ITO (∼17 Ω $\square^{-1}$)/PEDOT:PSS (30 nm)/P3OT:SWNTs (100 nm)/LiF (1 nm)/Al (80 nm), shown in figure 1(c), we obtain a V_{oc} value of 0.6 V, which is just equal to the difference between the value of HOMO level (5.4 eV) of P3OT [20] and the work function of SWNT (4.8 eV) [21]. Using electrochemical cyclic voltammetry, we calculated the lowest unoccupied molecular orbital (LUMO) (3.5 eV) and the HOMO (5.9 eV) of the PPE. The difference between the work function (4.8 eV) of SWNTs and the HOMO (5.9 eV) of the PPE is 1.1 eV, which agrees well with our experimental results (V_{oc} = 1.04 V).

Table 1. Electrochemical onset potentials and electronic energy levels of the PPE film.

Polymer	E^{ox}_{onset} (V versus Ag/Ag$^+$)	λ_{onset} (nm)	E^{opt}_g (eV)	HOMO (eV)	LUMO (eV)
PPE	1.15	517	2.40	−5.9	−3.5

In our experiment, the HOMO level for PPE is estimated using the oxidation potential of the polymer in the cyclic voltammetry curve (figure 2(a)), whereas the LUMO energy is extrapolated from this value by using the optical band gap ($E^{opt}_g = 1240/\lambda_{onset}$) in UV–vis absorption (figure 2(b)) [22]. Thus, the HOMO and LUMO of polymers were estimated according to the following equation [22]:

$$\text{HOMO} = -e(E^{ox}_{onset} - E_{Fc} + 4.8)(\text{eV}) \quad (1)$$

$$\text{LUMO} = \text{HOMO} - E^{opt}_g(\text{eV}), \quad (2)$$

in which

$$E_{Fc/Fc+} = 0.071\ V \text{ versus Ag/Ag}^+. \quad (3)$$

The results are summarized in table 1.

As can be seen from figure 1(c), the V_{oc} of the PPE/SWNTs device (1.04 V) is much higher than that of P3OT/SWNT based one (0.6 V). Usually, a high value of

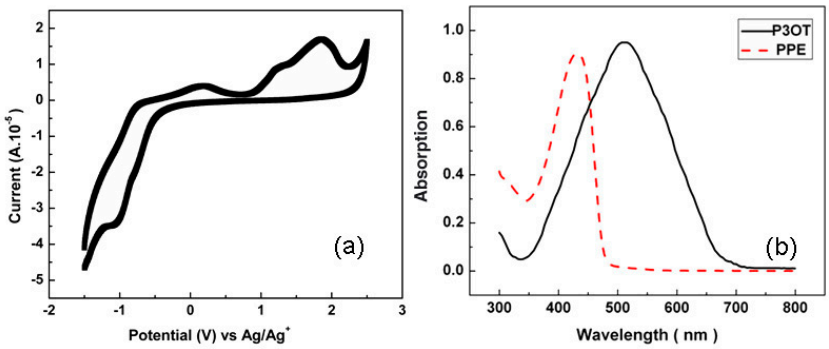

Figure 2. (a) Cyclic voltammograms of the PPE film on a platinum electrode in 0.1 M TBAP acetonitrile solution. (b) Absorption spectra of thin films of PPE (dashed line) and P3OT (solid line). The films were prepared by spin coating from solution in chloroform onto quartz substrates.

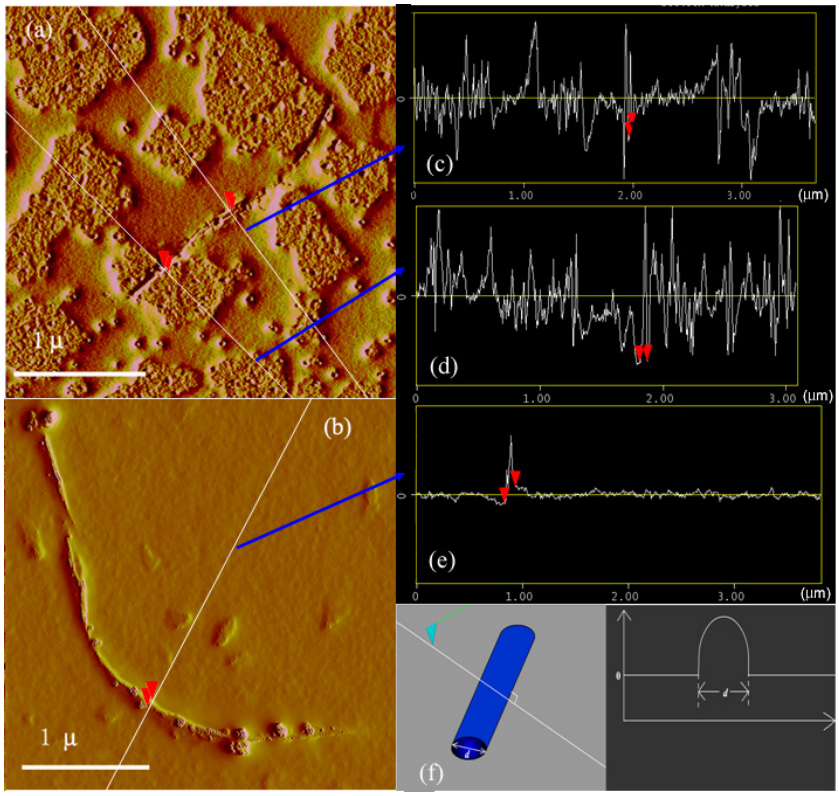

Figure 3. AFM pictures of PPE/SWNT (a) and P3OT/SWNT (b) composite film in tapping mode; using the 'section analysis' function of the AFM software, we measured the diameter of a thinner SWNT bundle in PPE ((c), 22 nm), an SWNT bundle in PPE ((d), 62 nm), and an SWNT bundle in P3OT ((e) 104 nm); the schematic representation of the 'section analysis' function is shown in (f). Typically, if there is a cylinder lying on a plane and we scan the plane across the cross section of the cylinder using an AFM tip (left image of (f)), we will obtain a curve representing the surface roughness (right image of (f)). Therefore the horizontal distance (d) in the right image is equal to the diameter (d) of the cylinder in the left image.

V_{oc} implies a high field in the heterojunction and then leads to a high dissociation efficiency of excitons into free charges, and can be favorable to the formation of the photocurrent. Besides V_{oc}, the distribution of SWNTs in the matrix strongly influences the charge transport and then the device performance of the bulk heterojunction structure of the photovoltaic device. To investigate the distribution of SWNTs in the PPE matrix and the P3OT matrix, the film morphologies of the composites were characterized using an atom force microscopy (AFM, Digital Instruments Inc., Nanoscope IV) in tapping mode, as shown in figure 3.

Figures 3(a) and (b) show SWNT bundles in a PPE matrix and in a P3OT matrix, respectively. Using the 'section analysis' function of the AFM software, we can obtain the diameter of the SWNT bundles in the PPE matrix and in the P3OT matrix; three examples are shown in figures 3(c)–(e). The schematic representation of the 'section analysis' function is shown in figure 3(f). Typically, if there is a cylinder lying

on a plane and we scan the plane across the cross section of the cylinder using an AFM tip (left image of (f)), we will obtain a curve representing the surface roughness (right image of (f)). Therefore the horizontal distance (d) in the right image is equal to the diameter (d) of the cylinder in the left image. We measured five points of the SWNT bundles in the PPE matrix and in the P3OT matrix in the AFM image and obtained the average value. It can be seen that an SWNT bundle with an average diameter of 65 nm was incorporated in the PPE matrix (e.g. figure 3(d)), with some part being separated into several thinner bundles of 22 nm diameter (e.g. figure 3(c)). Two SWNT bundles can be seen in figure 3(b) in the P3OT matrix with an average diameter of 105 nm (e.g. figure 3(e)) and thinner bundles can hardly be seen. Obviously SWNTs are more aggregated and poorly wet in the P3OT matrix than in the PPE matrix. The chemical structures of PPE, P3OT, and an SWNT are shown in figure 1(a). In our previous work [9] it was found that PPE and SWNTs interact strongly with each other and form a stable nano-hybrid, which may be caused by the structural similarity between PPE and SWNTs. From figure 3(a), it can be seen that PPE intersects into the SWNT bundle and separates the bundle into smaller ones, whereas we cannot seen similar thin SWNT bundles in the P3HT matrix in figure 3(b). This indicates that a better dispersion of SWNTs in a PPE matrix can be obtained compared with that in a P3HT matrix. A better dispersion of SWNTs will inevitably lead to more donor/acceptor (D/A) interfaces in the active layer, which facilitates the efficiency of exciton dissociation, provides more conducting channels for charge transfer and then leads to a high power conversion efficiency.

As we return to figure 1(c), we can see that PPE and P3OT based devices have similar J_{sc} values (0.25 mA cm^{-2} for PPE and 0.3 mA cm^{-2} for P3OT based devices). Besides the field of the D/A interface and the efficiency of dissociation and diffusion, which are influenced by V_{oc} and the SWNT distribution in matrix, the ability of harvesting solar energy is one of the important factors influencing J_{sc}, which is determined by the match of the absorption spectrum of the donor polymer with the solar spectrum. Therefore, we investigated the UV–vis spectroscopic properties of PPE and P3OT, as shown in figure 2(b).

From figure 2(b), it can be seen that PPE absorbs in the range 350–450 nm, while P3OT absorbs strongly over a wide range, 350–700 nm. As there is approximately 5% energy in the ultraviolet (300–400 nm) and 43% in the visible (400–700 nm) [23], PPE absorbs much less solar energy than P3OT. Considering the relatively weak absorption in the solar radiation of PPE compared with P3OT, it is reasonable that the J_{sc} of the PPE based photovoltaic device is not higher than that of the P3OT based one, despite the higher V_{oc} and better SWNT distribution in the PPE matrix.

5. Conclusion

A device using a PPE/SWNT active layer achieves almost the same J_{sc} as a P3OT/SWNT based one, and a higher value of V_{oc} compared with the P3OT based one. Furthermore, the overall power conversion efficiency of the PPE/SWNTs based device is 0.05%, higher than that of the P3OT based one (0.02%). The good dispersion of the SWNTs in PPE matrix make this composite a potential candidate in photovoltaic applications. At present, a limitation of the donor material (PPE) is its narrow absorption band, which hinders its photovoltaic performance, especially in J_{sc}. Such a problem can be overcome by introducing other functional groups into the backbone or side chain to improve the ability of harvesting solar energy. By broadening its absorption band, a higher J_{sc} and energy conversion efficiency can then be expected. This work is under progress.

Acknowledgments

The authors gratefully acknowledge the financial support from NSF (60676051, 20644004, 07JCYBJC03000) of China, Tianjin Natural Science Foundation (06TXTJJC14603), MoST (2006CB0N0702), and MoE (20040055020).

References

[1] Ishikawa T, Nakamura M, Fujita K and Tsutsui T 2004 *Appl. Phys. Lett.* **84** 2424
[2] Leger J M, Rodovsky D B and Bartholomew G P 2006 *Adv. Mater.* **18** 3130
[3] Koppe M, Scharber M, Duffy W, Heeney M and McCulloch I 2007 *Adv. Funct. Mater.* **17** 1731
[4] Carrasco-Orozco M, Tsoi W C, O'Neill M, Aldred M P, Vlachos P and Kelly S M 2006 *Adv. Mater.* **18** 1754
[5] Huynh W U, Dittmer J J and Alivisatos A P 2002 *Science* **295** 2425
[6] Shaheen S E, Brabec C J, Sariciftci N S, Padinger F, Fromherz T and Hummelen J C 2001 *Appl. Phys. Lett.* **78** 841
[7] Kim K, Liu J W, Namboothiry M A G and Carroll D L 2007 *Appl. Phys. Lett.* **90** 163511
[8] Dittmer J J, Marseglia E A and Friend R H 2000 *Adv. Mater.* **12** 1270
[9] Mao J, Liu Q, Lv X, Liu Z, Huang Y, Ma Y and Chen Y 2007 *J. Nanosci. Nanotechnol.* **7** 2696
[10] Palacios-Lidon E, Perez-Garcia B, Abellan J, Miguel C, Urbina A and Colchero J 2006 *Adv. Funct. Mater.* **16** 1975
[11] Warman J M, de Haas M P, Anthopoulos T D and de Leeuw D M 2006 *Adv. Mater.* **18** 2294
[12] Pradhan B, Batabyal S K and Pal A J 2006 *Appl. Phys. Lett.* **88** 093106
[13] Sgobba V, Rahman G M A, Guldi D M, Jux N, Campidelli S and Prato M 2006 *Adv. Mater.* **18** 2264
[14] Du F, Ma Y, Lv X, Huang Y, Li F and Chen Y 2006 *Carbon* **44** 1298
[15] Tohji K *et al* 1996 *Nature* **383** 679
[16] Umnov A G and Korovyanko O J 2005 *Appl. Phys. Lett.* **87** 113506
[17] Kim J Y, Kim S H, Lee H H, Lee K, Ma W, Gong X and Heeger A J 2006 *Adv. Mater.* **18** 572
[18] Parker I D 1994 *Appl. J. Phys.* **75** 1656
[19] Blom P W M, Mihailetchi V D, Koster L J A and Markov D E 2007 *Adv. Mater.* **17** 1551
[20] Salinas O H, López-Mata C, Hu H, Nicho M E and Sánchez A 2006 *Sol. Energy Mater. Sol. Cells* **90** 760
[21] Suzuki S, Bower C, Watanabe Y and Zhou O 2000 *Appl. Phys. Lett.* **76** 4007
[22] Mwaura J K, Pinto M R, Witker D, Ananthakrishnan N, Schanze K S and Reynolds J R 2005 *Langmuir* **21** 10119
[23] Kruse O, Rupprecht J, Mussgnug J H, Dismukesc G C and Hankamer B 2005 *Photochem. Photobiol. Sci.* **4** 957